"Unertan Syndrome" in two Turkish Families in Relation to Devolution and Emergence of Homo Erectus: Neurological Examination, MRI, and pet Scans

Üner Tan [a]; Sadrettin Pençe [b]; Mustafa Yilmaz [c]; Ayhan Özkur [d]; Sbel Karaca [e]; Melha Tan [e]; Mehmet Karata [e]
[a] Cukurova University, Faculty of Sciences, Department of Physics, Adana, Turkey [b] Medical School, Department of Physiology, Gaziantep University, Gaziantep, Turkey [c] Medical School, Department of Nuclear Medicine, Gaziantep University, Gaziantep, Turkey [d] Medical School, Department of Radiology, Gaziantep University, Gaziantep, Turkey [e] Medical School, Department of Neurology, Baskent University, Adana, Turkey

Online Publication Date: 01 March 2008

PLEASE SCROLL DOWN FOR ARTICLE

informa
healthcare

"UNERTAN SYNDROME" IN TWO TURKISH FAMILIES IN RELATION TO DEVOLUTION AND EMERGENCE OF HOMO ERECTUS: NEUROLOGICAL EXAMINATION, MRI, AND PET SCANS

ÜNER TAN

Cukurova University
Faculty of Sciences
Department of Physics
Adana, Turkey

SADRETTIN PENÇE

Gaziantep University
Medical School
Department of Physiology
Gaziantep, Turkey

Address correspondence to Prof. Dr. Uner Tan, Cukurova University, Faculty of Sciences, Department of Physics, 01330 Balcali Adana, Turkey E-mail: unertan37@yahoo.com E-mail: Uner.tan@gmail.com

MUSTAFA YILMAZ

Gaziantep University
Medical School
Department of Nuclear Medicine
Gaziantep, Turkey

AYHAN ÖZKUR

Gaziantep University
Medical School
Department of Radiology
Gaziantep, Turkey

SİBEL KARACA
MELİHA TAN
MEHMET KARATAŞ

Baskent University
Medical School
Department of Neurology
Adana, Turkey

"Unertan syndrome" consists of two main symptoms: quadrupedal gait and primitive cognitive abilities including language and conscious experience. To assess the central mechanisms involved in this syndrome, the authors performed MRI and PET scans on affected and unaffected individuals from both families. All affected individuals were also subjected to neurological examination. To assess the integrity of the peripheral and central vestibular system, Barany's caloric test was applied to the affected individuals. Brain MRI and PET scans were performed on normal subjects ($n = 7$) and patients ($n = 7$). Right- and left-cerebral and cerebellar areas, including the vermial and callosal areas, were measured on the MRI scans using a computer cursor. Quadrupedal gait, mental retardation, dysartric speech, nystagmus, severe truncal ataxia, hyperreflexia, astasia, and abasia were observed in the affected individuals from both families. Cerebellum and vermis were atrophic in the MRI and PET scans of the first family. In contrast, the brain MRI seemed to be normal in the MRI and PET scans of affected individuals from the second family. The caloric test revealed central vestibular damage in patients from the first family and peripheral vestibular damage in patients from the second family. The results suggest that "Unertan syndrome," discovered in two unrelated families, may be caused by peripheral or central vestibular damage resulting from different genetic defects. Cerebellar hypoplasia may not be a prerequisite for the emergence of this syndrome. Primitive mental abilities may be explained by damage within the vestibulo-cerebellar system, whereas the quadrupedal gait may be due

to a genetic defect within the higher brain centers that suppress the atavistic brain networks controlling quadrupedal gait and helped in the emergence of the habitual bipedal gait during human evolution. This retarded development of human locomotion—devolution—may illuminate the brain mechanisms responsible for the transition from quadrupedality to bipedality in human evolution.

INTRODUCTION

A new syndrome was first described by Tan in five siblings among 19 children in a family with intrafamilial marriage near Iskenderun, Turkey. The syndrome, referred to as "Unertan syndrome," consists of two main symptoms: quadrupedal palmigrade locomotion and primitive mental abilities, including primitive language and primitive conscious experience. The family was first evaluated on May 1, 2005. Since then, the discovery of "Unertan syndrome" in a second family has been reported in two articles (see Tan 2006b,c).

Genealogical analysis of the first and second families, found in a small village near the Syrian border and in Adana, respectively, suggested autosomal recessive transmission. Accordingly, genetic analysis of the first family revealed a single locus for homozygosity on chromosome 17p (Turkmen et al., 2006). This was confirmed in collaborative research with Ozcelik (unpublished observations). Interestingly, the affected individuals in the second family did not exhibit the same chromosomal anomaly. Therefore, the genetic defect on chromosome 17p does not seem to illuminate the origins of "Unertan syndrome." However, this does not exclude the single gene hypothesis, suggesting that a single gene may play a role in the transition from quadrupedality in human ancestors to bipedality in homo erectus (see Tan, 2005b; 2006a), because the candidate gene may be shared by several chromosomes.

Various congenital conditions exhibit symptoms more or less similar to those of "Unertan syndrome" such as Joubert Syndrome and sporadic Dandy-Walker malformation. In particular, the "dysequilibrium syndrome," an autosomal recessive condition prevalent in the Hutterite population of North America characterized by non-progressive cerebellar hypolasia and truncal ataxia, may be related to "Unertan syndrome." However, these two syndromes are mostly different from each other (see Table 1).

To reveal possible morphological changes in the brains of affected individuals, MRI scans were previously performed, indicating cerebellar, especially vermial atrophies in these patients (see Tan, 2005b; 2006a; Turkmen

Table 1. Differences between "Unertan syndrome" and "dysequilibrium syndrome"

Traits	"Unertan Syndrome"	"Dysequilibrium"
Transmission	Autosomal recessive	Autosomal recessive
Defect	17p (1st family); no 17, no 9(2nd family)	9p
Gait	Always quadrupedal	Bipedal ataxic
Ataxia	Severe truncal	Severe truncal
Stance	Usually broad-based	Always borad-based
Tendon reflex	Usually brisk	Always brisk
Hand tremor	Sometimes	Always
Nystagmus	Yes	No
Dysmetria	Yes	Yes
Hypotonia	No	Yes
Dysarthria	Yes	No
Mental retar.	Severe to mild	Mild to moderate
Cereb. atr.	Not always	Always
Vermial atr.	Not always	Always
Ves. disorder	Central or peripheral	Central
Short stature	No	Yes

Mental Retar.: mental retardation; Cereb. Atr.: cerebellar atrophy; VERMIAL ATR.: vermial atrophy; Ves. Disorder: vestibular disorder.

et al., 2006). However, these papers presented just one MRI scan from only one person, and there were no control scans from the normal individuals in the same family. Furthermore, no brain MRI examinations had been conducted on the second family, about which only one article has been published (Tan, 2006c). For these reasons, the present study took brain MRIs from affected and unaffected individuals in both families. In addition, positron emission tomography (PET) scans were used to examine glucose utilization by cerebral and cerebellar neurons in these subjects. Interestingly, the MRI and PET scans seemed to be normal in both affected and non-affected individuals from the second family, whereas the cerebellum and especially the cerebellar vermis showed a high degree of hypoplasia and very low metabolic activity in affected individuals from the first family.

MATERIALS AND METHODS

Participants

Two families exhibiting "Unertan syndrome" have been described in five recent articles (Tan 2005a, b; Tan 2006a, b, c). The participants in the present study

were 5 quadrupedal, 1 bipedal-ataxic, and 7 bipedally normal individuals from the first family (mean age $= 28.4 \pm 6.3$), as well as 1 quadrupedal man, 27 years old, 1 bipedal-ataxic man, 33 years old, and 1 bipedally normal man, 30 years old, from the second family. The study was approved by the ethical committee of the Medical School of Cukurova University, and all participants provided written consent prior to examinations. The participants were not taking any medicine that could influence neural excitability.

Neurological Examination

On neurological examination, the authors looked for horizontal and/or vertical nystagmus to assess any dysfunction within the vestibulo-cerebellar system connecting the vestibular system with the floccolonodular lobe of cerebellum. Truncal stability during sitting and standing was examined to assess the spinocerebellar system. Ataxic syndromes caused by vestibulocerebellar and spinocerebellar disease (midline ataxias) indeed show truncal instability and gait ataxia (wide-based walking). The cranial nerves, muscle tone, muscle strength, coordination and gait (rapid alternating movements, point to point movements), Romberg gait, deep tendon reflexes, clonus, plantar response (Babinsky), vibration, and position senses were also examined.

To assess the function of the peripheral and/or central vestibular system, Barany's caloric test was performed. During this standard clinical test the subject was reclining, head inclined 30 degrees from horizontal, so as to make the lateral canal horizontal. Water was introduced through a plastic tube into the ear canal, $7°C$ below body temperature, for 30 s, then nystagmus was observed away from the stimulated side. The duration of nystagmus was recorded; it normally decays within 2 min. This procedure was performed separately for the right and left ears. During caloric vestibular stimulation, the vestibular cortex within the posterior insula and retroinsular region is activated, and the visual cortex is bilaterally reactivated (Bense et al., 2004).

Magnetic Resonance Imaging (MRI)

Patients were scanned with a Siemens (Erlangen, Germany) 1.5 T magnetic resonance scanner using a standard head coil and a tilted T1-weighted coronal and sagittal sequence and a T2-weighted axial spin-echo sequence. The participants were asked to remove anything that might degrade MRI images of the head, such as hairpins, jewelry, eyeglasses, and hearing aids, before the MRI was performed, and were then placed on a sliding table so that the surface

coil was positioned around the head. After positioning the individuals with the head inside the MRI gantry, the radiologist and technologists left the room and the MRI sequences were performed. The individuals were asked not to move during the imaging process but were able to communicate with the radiologist at any time using an intercom.

The region of interest was traced manually by a single tracer, blinded to the clinical data and diagnostic category, using a workstation (Sun Microsystems Inc., Mountain View, CA, USA) and commercially available software for image analysis (Magic View 1000, Siemens). Total areas (mm^2) of the vermis, cerebellar hemispheres, cingulate gyrus, lentiform nucleus, and thalamus were obtained by outlining these structures on coronal and sagittal slices. The cerebellar vermis and corpus callosum were traced on the midsagittal section. The cerebellar hemispheres were traced on the coronal sections, excluding vermis, cerebellar peduncles, and the fourth ventricle. The lentiform nucleus and thalamus were traced on the axial section. The areas were computed using Java software. Figure 1 illustrates the areas of sagittal (above) and coronal brain sections (below) measured. The measured areas above in Figure 1 are the cerebral hemisphere (A), corpus callosum (B), and cerebellum (C); below, right-cerebral hemisphere (A), left-cerebral hemisphere (B), right-cerebellum (C), and left-cerebellum (D).

Positron Emission Tomography (PET)

The PET scans were performed in the Department of Nuclear Medicine of the Medical School of Gazi Antep University to examine brain metabolic activity in the normal and affected participants. The participants were required not to smoke or drink caffeine or alcohol for 24 h, or to eat or drink anything for 8 h, before the test.

Brain FDG-PET imaging was performed with a dual-modality PET/CT system (Biograph 2, Siemens Medical Solutions USA, Inc., Hoffman Estates, IL). The Biograph 2 scanner consists of a combination of a dual-slice spiral CT and a high resolution PET scanner with a 16.2 cm axial field of view and a plane spacing of 3.4 mm. Patients and normal family members fasted for at least 4 h. They received an intravenous injection of 362.6 ± 59.2 MBq [18] F-FDG (fluorodeoxyglucose) in a quiet, dimly lit room; subjects had their eyes open and ears unoccluded and they remained in this environment for 60 min. Blood glucose level measured prior to injection was 104 ± 17.7 mg/dl. The mother was excluded from this part of the study because of a high blood glucose level (310 mg/dl).
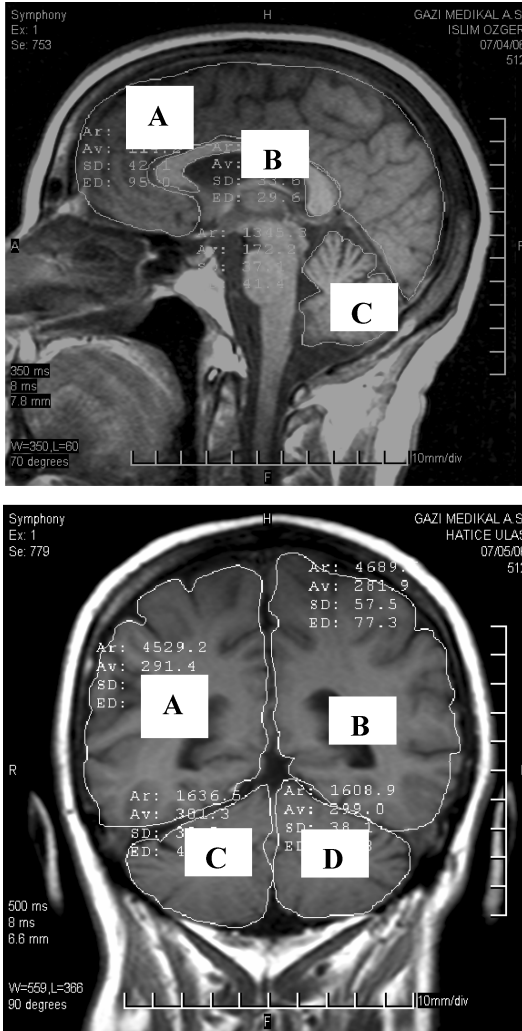
Figure 1. Measured areas in MRI. Above: sagittal section; A, cerebrum; B, corpus callosum; C, cerebellar vermis. Below: coronal section; A, right-cerebral hemisphere; B, left-cerebral hemisphere; C, right-cerebellar hemisphere; D, left-cerebellar hemisphere.

PET/CT imaging was started 60 min after FDG administration. Cranial CT imaging was performed before PET imaging to correct attenuation and for anatomical localization. Then brain PET imaging was performed for 10 min with the subjects' heads immobilized by a strap on the scanner bed.

Attenuation-corrected PET images were reconstructed with an ordered subset expectation maximization iterative reconstruction algorithm. PET slices were evaluated visually and semiquantitatively on the transaxial, coronal, and sagittal planes. Brain glucose utilization was expressed by SUV, which is the standardized uptake value of FDG.

Written informed consent was obtained from all participants. The study was approved by the ethics committee of the Medical School, Cukurova University (Adana, Turkey), in accordance with the Helsinki declaration.

RESULTS

Neurological Examination

The results of the neurological examinations of the two families are presented in Table 2. Two men in both families were quadrupedal during childhood and biped-ataxic during adulthood. The common symptoms were quadrupedal palmigrade locomotion, mental retardation, dysartric speech using fewer than a hundred words, primitive conscious experience (see Tan 2005a, b; Tan, 2006a, b, c). The man in the first family did not use broad-base walking in his quadrupedal gait. Nystagmus and dysdiadocokinesis were observed in all cases. There was hyperexcitability (>3 min) in the Barany's caloric nystagmus test in the affected members of the first family, but no response, that is, no nystagmus, in the affected individuals of the second family.

MRI Examinations

Correlations between Body Size and Cerebral Areas. There were 14 participants from the 2 families: 7 controls and 7 patients. Body size correlated significantly with areas in the sagittal and coronal MRI scans of the brain (Table 3): body height and weight correlated significantly with the right- and left-cerebral areas, right- and left-cerebellar areas, vermial, and callosal areas; there were also significant correlations among the cerebral, cerebellar, vermial, and callosal areas.

MRI Scans of the First Family

In all the affected individuals there was cerebellar and especially vermial atrophy with wide cerebellar and vermial sulci, and mild atrophy of the parietal cortex and corpus callosum, especially in the splenium and corpus regions

Table 2. Neurological findings in the affected members of the first and second families

Examinations	1st family	2nd family
Gait	Quadrupedal (5/6)	Quadrupedal (1/2)
Broad-based gait	in 4 of 5	in 2 of 2
Astasia	Yes	Yes
Abasia	Yes	Yes
Mental retardation	Mild	Mild
Speech	Dysartric	Dysartric
Truncal ataxia	Yes	Yes
Nystagmus	Yes	Yes
Dysmetria	Yes	Yes
Dysdiadocokinesis	Yes	Yes
Babinsky	+ (3/5)	(–)
Hoffman	+ (3/5)	(–)
Tendon reflexes	Hyperactive	Hyperactive in legs
Caloric test	Nystagmus > 3 min	No response

(callosal dyskinesia). The basal ganglia, thalamus, bulbus, and pons appeared to be normal. The mean areas of the right- and left-cerebral and cerebellar hemispheres, vermis and corpus callosum of control subjects and affected individuals are presented in Table 4.

Right- and Left-Cerebral Areas. Univariate analysis of variance indicated that the mean right-cerebral area is significantly smaller in affected individuals

Table 3. Correlation coefficients among body height and cerebral areas in MRI

Structures	Height	Weight	R-cereb.	L-cereb.	R-cerebel.	L-cerebel.	Vermis	CC
Height	—	.35	.81**	.69**	.80**	.83**	.66**	.54*
R-cerebrum	.81**	.84**	—	.90**	.75**	.79**	.78**	.64*
L-cerebrum	.69**	.94**	.90**	—	.72**	.79**	.77**	.66**
R-cerebel.	.80**	.56*	.75**	.72**	—	.95**	.92**	.78**
L-cerebel.	.83**	.70**	.79**	.79**	.95**	—	.91**	.74**
Vermis	.66*	.67**	.78**	.77**	.92**	.91**	—	.84**
Corpus cal.	.54*	.58*	.64*	.66**	.70**	.74**	.83**	—

**Correlation is significant at the 0.01 level (2-tailed); *Correlation is significant at the 0.05 level (2-tailed); R-cereb.: right-cerebral area; L-cereb.: left-cerebral area; R-cerebel.: right-cerebellar area; L-cerebel.: left-cerebellar area; CC, callosal area.

Table 4. Cerebral and cerebellar areas in controls and affected imdividuals

Areas (mm^2)		Control subjects					Affected individuals			
	N	Mean	SD	Min	Max	N	Mean	SD	Min	Max
Cerebrum										
Right	7	4919.3	578.0	4246.7	5931.0	5	3932.1	513.9	3465.6	4531.0
Left	7	4750.6	476.1	4027.0	5531.0	5	3891.6	327.0	3531.0	4284.0
Cerebellum										
Right	7	1669.9	109.5	1521.0	1853.5	5	1113.7	16.8	1092.5	1130.0
Left	7	1568.5	120.0	1431.0	1765.1	5	1102.0	27.9	1076.3	1142.5
Vermis	7	1280.8	251.5	931.0	1726.5	5	436.8	55.8	344.0	494.3
Corpus callosum	7	640.0	111.2	547.7	818.2	5	425.2	85.3	334.7	529.9

than in unaffected close relatives ($F_{1, 10} = 9.3, p = .01$). However, because the right-cerebral area correlated directly with body height, the univariate analysis was repeated with height as covariate. This decreased the mean right-cerebral area to 4558.8 mm^2 ($SE = 215.1$) in controls and increased it to 4436.8 mm^2 ($SE = 274.4$) in the patients, and the difference was not statistically significant ($F_{2, 9} = 0.1, p > .75$). Similarly, the left-cerebral area was found to be significantly smaller in patients than in controls ($F_{1, 10} = 12.0, p < .01$, eta squared = 0.55). Again, because there was a direct correlation between the body height and the left-cerebral area, the univariate analysis of variance was repeated with height as covariate. This decreased the left-cerebral area to 4562.3 mm^2 ($SE = 195.2$) in controls and increased it to 4155.2 mm^2 ($SE = 248.9$) in the patients, and the difference was not statistically significant ($F_{2, 9} = 1.2, p > .30$). The controlled value of body height was 160.0 cm for the right- and left-cerebral areas.

Cerebellum. The body height was found to be directly related to the right- and left-cerebellar areas: for height versus right-cerebellar area, $r = 0.85$, $r^2 = 0.73$, $F_{1, 10} = 26.6, p < .001$; for height versus left-cerebellar area, $r = 0.83$, $r^2 = 0.69$, $F_{1, 10} = 21.7, p < .001$. Univariate analysis indicated that the mean right-cerebellar area was significantly smaller in affected than in unaffected individuals (see Table 4; $F_{1, 10} = 140.7, p < .001$, eta squared = 0.93). Taking the body height as a covariate did not change this finding ($F_{2, 9} = 46.1, p < .001$, eta squared = 0.84). The mean area of the left-cerebellar area was also found to be significantly smaller in affected than in non-affected individuals (see Table 4; $F_{1, 10} = 72.2, p < .001$, eta squared = 0.88). Taking the body height as a

covariate did not materially alter this result ($F_{2,9} = 19.1$, $p < .005$, eta squared $= 0.68$) taking body height as 160.0 cm.

Figure 2 shows the cerebral structures in the T1-weighted sagittal brain scans, normals (A: mother, B: father, and C: daughter) on the left column, affected individuals (D: daughter, E: son, and F: another daughter) on the right. The ratios of cerebellar to cerebral areas in these sections were 35.2%, 32.6%, and 34.4% for the mother, father, and daughter, respectively. The corresponding values for the patients were 24.6%, 28.2%, and 29.2%. The mean cerebellar to cerebral area ratio was 0.48 ± 0.12 in the unaffected control subjects from the same family, and 0.31 ± 0.02 in the affected individuals. This difference was significant ($F_{1,10} = 8.75$, $p < .05$, eta squared $= 0.47$).

Cerebellar Vermis. There was a direct correlation between vermial area and body height ($r = 0.78$, $r^2 = 0.61$, $F_{1,10} = 15.8$, $p < .005$). The mean vermial area was significantly greater in the unaffected than in the affected individuals (see Table 4; $F_{1,10} = 53.0$, $p < .001$, eta squared $= 0.84$). Taking the body height as a covariate did not materially alter this result ($F_{2,9} = 14.4$, $p < .005$, eta squared $= 0.62$).

The very small vermis in the affected individuals is clearly illustrated in Figure 3, which shows the midsagittal MRI scans. Unaffected family members are shown on the left (A: mother, B: father, C: daughter) and affected ones on the right (D: daughter, E: son, F: another daughter). The mean ratios of the vermial to the cerebral areas were 0.15 ± 0.04 in the controls ($n = 7$) and 0.06 ± 0.01 in the affected individuals ($n = 5$), the difference being highly significant ($F_{1,10} = 31.42$, $p < .0001$, eta squared $= 0.76$).

Corpus Callosum. The mean callosal area was significantly smaller in affected individuals than in controls (see Table 4; $F_{1,10} = 13.1$, $p = 0.005$, eta squared $= 0.57$). There was a direct relationship between the callosal areas and the body heights in the overall sample ($r = 0.76$, $r^2 = 0.58$, $p < 0.005$). When height was taken as a covariate, the mean callosal area increased to 524.7 mm^2 (SE $= 65.7$) in the patients and decreased to 583.3 mm^2 in the controls; it was still smaller in the patients, but the difference was not statistically significant ($F_{2,9} = 0.34$, $p > 0.55$). The mean ratios of the callosal area to the midsagittal cerebral area were 0.08 ± 0.02 for the control subjects and 0.06 ± 0.01 for the patients, the difference being marginally significant ($F_{1,10} = 4.82$, $p = 0.05$, eta squared $= 0.33$).

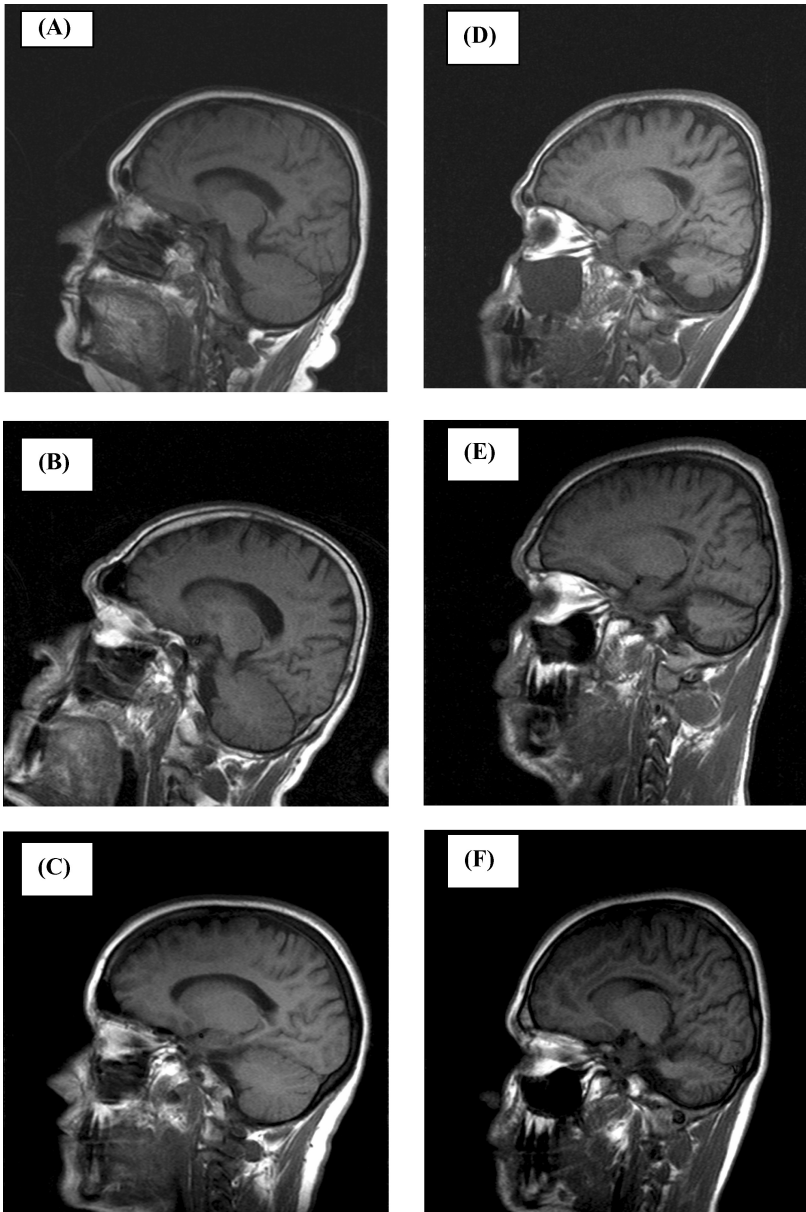**Figure 2.** Sagittal brain scans to visualize the cerebellum from mother (A), father (B), unaffected daughter (C), affected daughter (D), affected son (E), and another affected daughter (E).
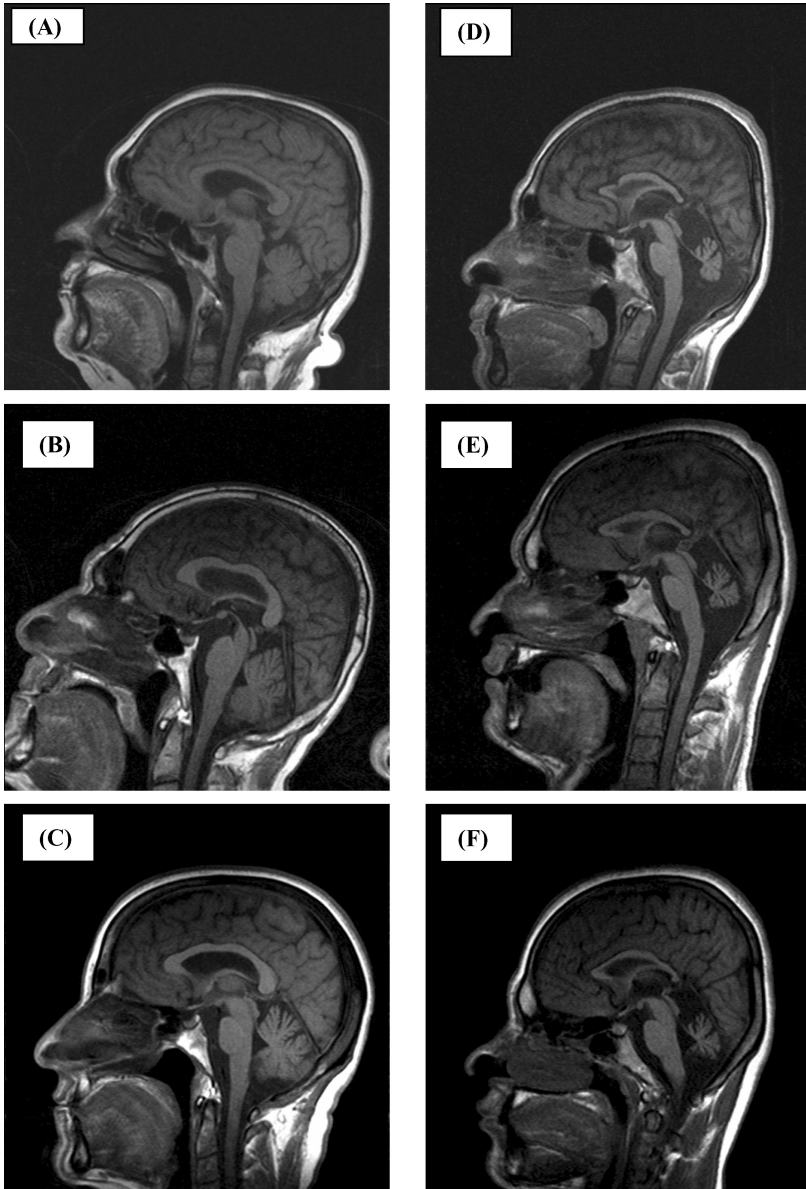
Figure 3. Midsagittal MRI scans to visualize the cerebellar vermis, cerebrum, and corpus callosum from mother (A), father (B), unaffected sister (C), affected daughter (D), affected son (E), and another affected daughter (F).

MRI Scans of the Second Family

The sagittal brain scans are shown in Figure 4. There were no cerebellar (left) and vermial (right) atrophies in the quadrupedal man (B, E) or the bipedal-ataxic man (C, F) compared to the control subject (A, D). Accordingly, the ratios of cerebellar to cerebral area in the coronal sections were 0.30 and 0.36 in the quadrupedal and bipedal men, respectively. These ratios were very close to 0.30 in the control subject.

The ratios of vermial to cerebral areas in the midsagittal sections were 0.23 in the quadrupedal man, which is close to 0.19 in the control subject, and 0.13 in the bipedal-ataxic man, which is smaller than the control. The cerebral cortex exhibited mild atrophy with widened sulci, especially in the frontal cortical areas. The basal ganglia, thalamus, bulbus, and pons seemed to be normal. There was a mild atrophy in the corpus callosum.

PET Scans

First Family. The mean glucose metabolic rates, SUVs, for the control and patient groups are presented in Table 5. The rate was significantly lower in the patients ($F_{1,10} = 13.23$, $p = .005$, partial eta squared = 0.57, for the right cerebellum; $F_{1,10} = 28.45$, $p < .001$, partial eta squared = 0.74, for the left cerebellum; $F_{1,10} = 48.83$, $p < .001$, partial eta squared = 0.83, for the cerebellar vermis). There were no significant differences between the mean SUVs for the remaining cerebral structures ($F_{1,10} = 0.11$ to 1.77, $p > .70$ to .20).

Figure 5 depicts the PET scans from four members of the first family. The metabolic activity seems to be normal in all brain regions of the father (A) and a normal daughter (C), whereas it is clearly decreased in the cerebellum and to a lesser extent in the cerebral cortex in the affected individuals (B, D). The basal ganglia and thalamus show normal metabolic activity.

Second Family. Figure 6 depicts the sagittal (left-column) and coronal (right-column) PET scans of brains from members of the second family. At the top is a normal family member (A, D) with normal metabolic activities in the cerebrum, cerebellum, caudate nucleus, and thalamus. Figure 6B and E show the sagittal (B) and coronal (E) PET scans of the quadrupedal man, whereas Figure 6C and F show the FDG uptake in the bipedal-ataxic man.

In the quadrupedal man, the FDG uptake seemed to be slightly increased in most brain regions compared to the control subject and the bipedal-ataxic
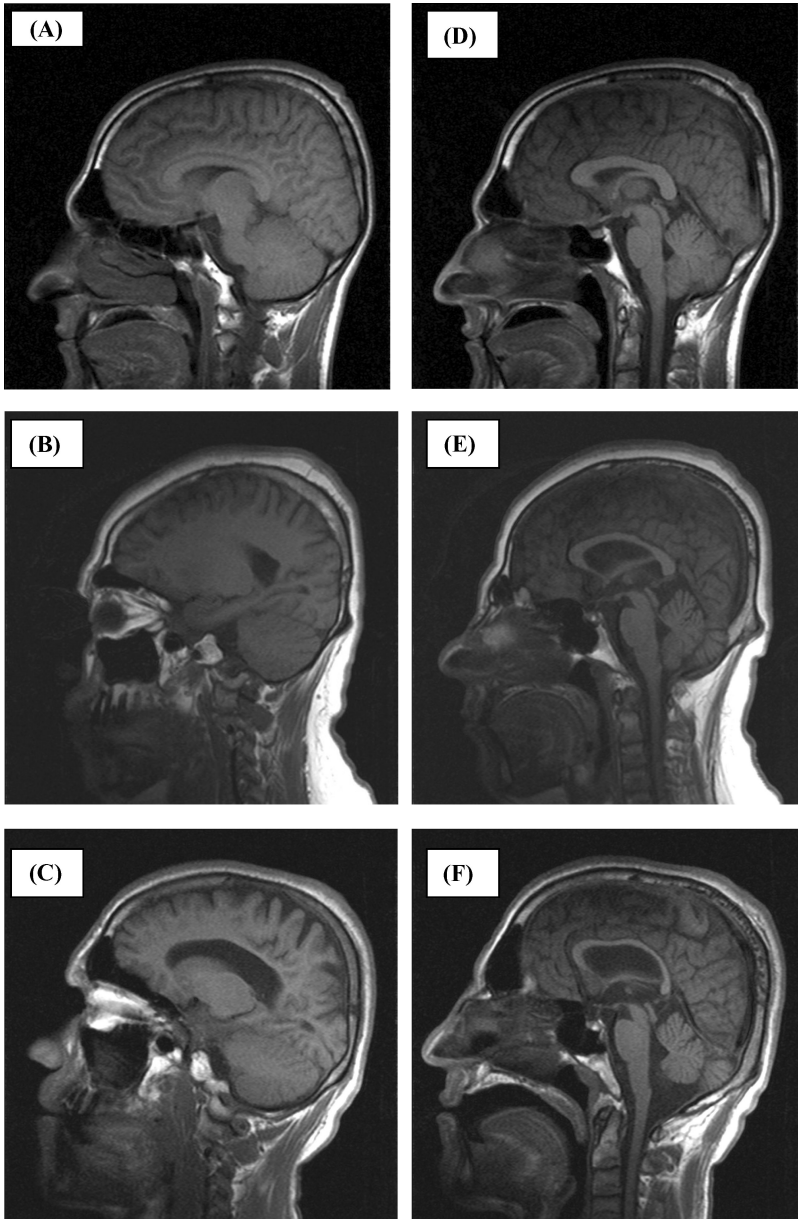
Figure 4. Sagittal MRI scans from a control subject (A, D), the quadrupedal man (B, E), and the bipedal-ataxic man (C, F) from the second family. Notice the normal cerebellum in all subjects (left column) and the mild vermial atrophy in the affected individuals (right column).

Table 5. Mean SUVs in controls and patients

| Cerebral structures	N	Mean	SD	SEM	Minimum	Maximum
Right cerebellum						
Controls	7	7.99	2.00	0.76	5.31	10.30
Patients	5	4.54	0.73	0.33	3.70	5.50
Left cerebellum						
Controls	7	7.91	1.42	0.53	5.81	9.50
Patients	5	4.20	0.72	0.32	3.60	5.30
Cerebellar vermis						
Controls	7	8.33	1.30	0.49	6.11	9.60
Patients	5	4.04	0.46	0.21	3.40	4.75
Right thalamus						
Controls	7	12.29	1.49	0.56	10.20	14.31
Patients	5	12.60	1.71	0.76	10.60	15.10
Left thalamus						
Controls	7	11.72	1.29	0.49	9.80	14.01
Patients	5	12.44	1.59	0.71	10.40	14.75
Right basal ganglia						
Controls	7	12.55	1.29	0.49	11.10	14.31
Patients	5	13.12	1.50	0.67	12.10	15.70
Left basal ganglia						
Controls	7	12.43	1.22	0.46	10.89	14.31
Patients	5	12.88	1.56	0.70	11.70	15.55
Right occipital cortex						
Controls	7	13.95	1.92	0.73	12.00	16.31
Patients	5	14.12	2.44	1.09	11.41	18.00
Left occipital cortex						
Controls	7	13.65	1.99	0.75	11.00	16.00
Patients	5	13.96	1.99	0.75	11.00	16.00
Right frontal cortex						
Controls	7	12.56	1.14	0.43	11.00	14.00
Patients	5	11.42	2.13	0.95	8.60	14.50
Left frontal cortex						
Controls	7	12.61	1.23	0.47	11.00	14.00
Patients	5	11.38	1.98	0.89	8.60	14.00
Right parietal cortex						
Controls	7	10.77	1.39	0.53	9.00	12.50
Patients	5	10.58	2.20	0.98	7.55	13.50
Left parietal cortex						
Controls	7	11.01	1.24	0.47	9.30	12.55
Patients	5	10.30	1.86	0.83	7.50	12.50
Right temporal cortex						
Controls	7	11.00	0.95	0.36	9.50	12.33
Patients	5	9.90	2.13	0.95	7.00	13.00
Left temporal cortex						
Controls	7	10.79	0.94	0.36	9.30	12.11
Patients	5	10.06	1.86	0.83	7.50	12.50
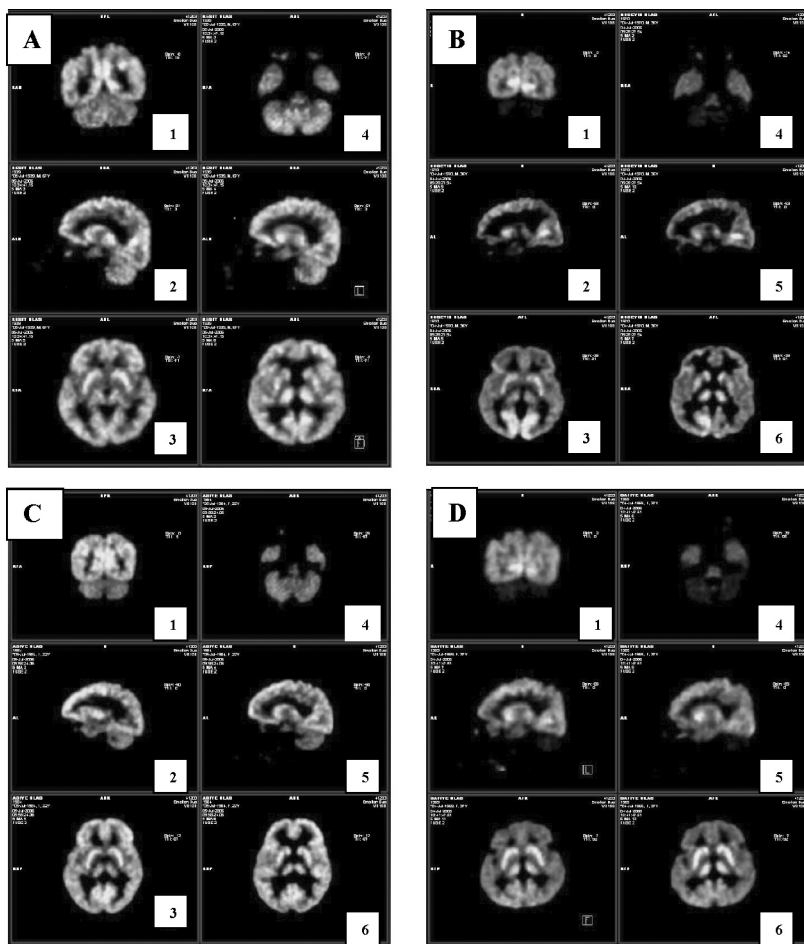
Figure 5. PET scans from four members of the first family. A, father; C, normal daughter; B, quadrupedal son; D, quadrupedal daughter. 1, coronal section through occipital cortex and cerebellum; 2, sagittal section through right-hemisphere, right-cerebellum; 3, transaxial section through putamen; 4, transaxial section through inferior temporal cortex, cerebellum; 5, sagittal section through left-hemisphere, left-cerebellum; 6, transaxial section through thalamus.

man (Table 2). That is, his cerebellum, vermis, frontal cortex, parietal cortex, temporal cortex, and occipital cortex were slightly hypermetabolic compared to the others. The overall brain metabolic activity seemed to be slightly decreased in the bipedal-ataxic man (Table 6).

Table 6. Mean glucose metabolic rates (SUV) in second family

Subjects	Cerebel.			Frontal		Parietal		Temp.		Occipit.		Basal g.		Thalam.	
	R	L	Ver.	R	L	R	L	R	L	R	L	R	L	R	L
Normal	9.8	9.1	9.3	12.7	12.8	12.5	10.8	10.3	10.0	13.34	14.0	13.3	12.3	14.3	12.3
Quadr.	12.5	13.2	14.3	14.0	14.5	13.5	13.5	12.0	12.0	19.2	18.9	13.8	14.4	14.0	13.7
Biped.	9.2	8.9	8.8	10.5	10.3	10.0	10.0	9.0	8.1	11.0	10.7	10.5	10.6	10.1	9.9

Quadr., quadrupedal man; biped, bipedal-ataxic man; cerebel., cerebellum; ver., vermis; frontal, frontal cortex; parietal, parietal cortex; temp., temporal cortex; occipit., occipital cortex; basal g., basal ganglia, thalam., thalamus; R, right; L, left.
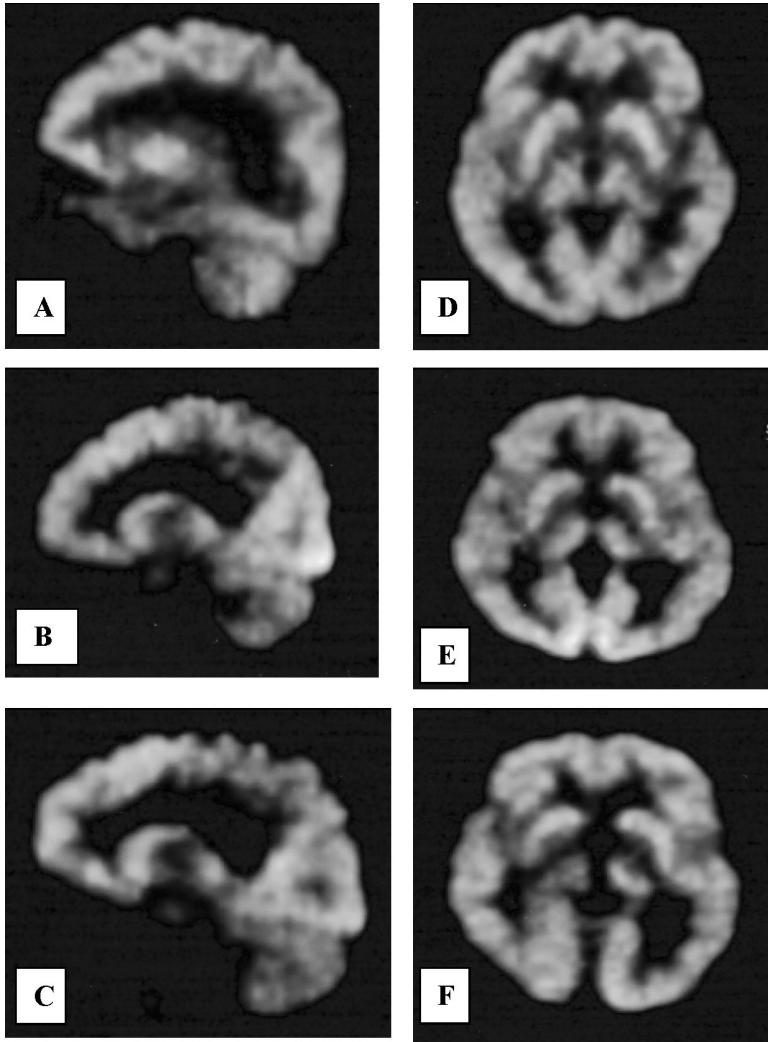
Figure 6. Cerebral PET scans from members of the second family. Left, sagittal; right, transaxial sections. A, D: control subject, a family member; B, E: quadrupedal man; C, F: bipedal-ataxic man.

DISCUSSION

The authors studied MRI and PET scans of the affected and unaffected members of the two families to elucidate the origins of "Unertan syndrome." The families shared some genealogical traits such as intra-familial marriages

and showed similar symptoms such as quadrupedal palmigrade locomotion, retarded intelligence, and primitive language abilities (Tan, 2005a, b; Tan, 2006a, b, c). However, different genetic defects were probably responsible for this condition in the two families, because a defect was found in chromosome 17p in the first family, but a different chromosomal defect in the second family (Ozcelik et al., unpublished observations). The caloric nystagmus test also revealed that a central vestibular defect may be present in the first family, but a peripheral vestibular defect in the second. These results suggest that "Unertan syndrome" may be a disorder of the vestibular system.

Consistent with the different but closely related origins of this syndrome, the authors obtained different results from the MRI and PET scans of affected members of the two families. The study measured various cerebral and cerebellar areas on the MRI scans expecting that they would provide volumetric measurements of these regions, because cerebral areas measured on MRI scans correlate significantly with cranial volume in human male and female subjects (Tan et al., 1999). In the first family, the right- and left-cerebral and cerebellar areas were significantly smaller in the affected than in the unaffected individuals. Because these areas correlated significantly with body height, ANOVA was performed, taking body height as a covariate. This showed that the cerebral and cerebellar areas remained smaller in the affected than the unaffected individuals but the difference was statistically insignificant. However, cerebellar metabolic activity was barely detectable in the PET scans of affected individuals, that is, the PET scan emphasized the cerebellar hypoplasia. These results suggest that the cerebellum is affected morphologically and metabolically in these subjects.

The vermial area was also significantly smaller in the affected than the unaffected individuals of the first family. Because the vermial area correlated significantly with body height, ANOVA was again performed, taking body height as a covariate. The vermial areas remained significantly smaller in the affected individuals. These results suggest that genetic defects in the cerebellum and especially the cerebellar vermis may play a role in the origin of "Unertan syndrome" in members of the first family.

Quadrupedal gait does not seem to be related to cerebellar or vermial atrophy, because several studies have shown that human cerebellar damage produces abnormalities of balance and locomotion (Earhart & Bastian, 2001) and no study prior to the recently identified "Unertan syndrome" had described quadrupedal palmigrade locomotion resulting from cerebellar damage in humans. Furthermore, a bipedal-ataxic man showed MRI and PET results similar to those from the quadrupedal individuals.

The retarded cognitive abilities, including language, may be related to the cerebellar and vermial hypoplasia because these structures play a role in higher cognitive functions including language. Anatomically, the cerebellum is connected to the cortical association areas subserving cognition, and the vermis is connected to limbic structures including the hippocampus and amygdala (Schmahmann, 1996). Functionally, language processing and verbal working memory tasks activate some regions of the cerebellum (Leiner et al., 1995). The cerebellum indeed contributes to higher cognitive activities such as language, thought modulation, emotions, and the ability to organize symbolic activities (Schmahmann, 1991; Fiez et al., 1992; Leiner et al., 1993). Therefore, retarded linguistic and other cognitive abilities may be expected to result from the cerebellar damage found in the affected individuals of the first family.

In contrast to the hypometabolic and atrophic cerebellum and vermis in affected individuals of the first family, these structures seemed to be normal in affected individuals of the second family. Accordingly, the caloric nystagmus test indicated a central vestibular defect (e.g., cerebellum) in the first family and a peripheral vestibular defect (e.g., semicircular canals, otoliths, hair cells, vestibular nerve) in the second family. The peripheral and central vestibular systems, two closely related neural networks, are known to play a role in posture and balance. Therefore, they may have caused the similar symptoms observed in the two families.

Despite the genetic and morphological differences between the two families, the affected members of both exhibited the main symptoms of "Unertan syndrome." A normal cerebellum in the second family, and the cerebellar and vermial atrophy in the bipedal-ataxic man of the first family, suggest that quadrupedal palmigrade locomotion has nothing to do with cerebellar damage. However, this does not mean that quadrupedal gait in humans is a psychological variable depending on individual preference. There must, of course, be a developmental defect in the brain that interrupts the normal transition from quadrupedal crawling during babyhood to the bipedal upright walking of childhood. Interestingly, it has recently been reported that a man who had poliomyelitis during babyhood rejected all encouragement to walk upright, preferring the quadrupedal walking pattern during childhood and adulthood. His brain, including the cerebellum, seemed to be quite normal in MRI; his cognitive abilities, including language, seemed even to be above normal (Tan, 2007); there was no intra-familial marriage and no genetic transmission. Probably the polio virus had damaged the brain networks responsible for the transition from bear-crawling to upright bipedal walking. As in the first and second families, MRI may be insufficient to show minor changes within the

brain. A similar case after polio was observed in the Canary Islands (e-mail report). The patient seemed to be mentally normal. A man in the United States has reported to me that "I was up there for football camp and on the way back from a practice, we saw them running the hill. It was insane . . . they are supposed to go up and down the hill five times in five minutes (not sure if it was multiple sets). While we were walking by, there were three or four guys basically bear crawling their way up" (correspondence by e-mail). A friend of mine saw a man hurrying up across the street on all fours; he disappeared quickly. These quadrupeds seemed to be mentally quite normal. Thus, some normal people prefer wrist-walking during adulthood. The aforementioned sporadic wrist-walkers do not apparently exhibit "Unertan syndrome," which is a combination of two main symptoms: quadrupedal gait and primitive cognitive abilities including language and conscious experience.

The quadrupedal gait is seen from time to time in some children, but they stand up and start to walk on two feet, achieving a bipedal gait for the rest of their life. On the other hand, there may be adult wrist-walkers with apparently normal brain structures and normal intelligence. As mentioned earlier, quadrupedal wrist-walking may appear sporadically, independently of the other symptoms of "Unertan syndrome." There may be other defects within the higher brain centers in these cases. During normal development of babies, some stages consist of creeping, normal crawling, or, more rarely, bear-crawling, and finally the upright stance with bipedal gait. Individual humans may thus experience all the stages in the evolution of human locomotion. However, in some rare cases, motor development may stop at the bear-crawling stage, and these individuals prefer wrist-walking for the rest of their lives. Thus, normal development of locomotion may be interrupted somewhere between quadrupedal and bipedal gait and the quadrupedal gait stage cannot be superseded. That is, motor development in these cases may stop at the quadrupedal locomotion stage, suggesting a retarded or reverse evolution, showing an atavistic feature. This may be genetic and/or environmental in origin. For the genetic origin, there is evidence in the literature that reverse evolution is possible (Porter & Crandall, 2003). For the environmental origin, there are quadrupedal wrist-walkers as a result of poliomyelitis (see Tan, 2007).

The cerebral networks responsible for the development of upright stance and bipedal walk, simultaneously repressing the ancestral spino-cerebral motor mechanisms inducing qaudrupedal gait, may be absent or not fully developed during early babyhood in the sporadic quadrupedal individuals. These cases would be highly informative as a live model for the transition from quadrupedality to bipedality during human evolution.

CONCLUSION

This article presented two families exhibiting "Unertan syndrome," emphasizing the neurological examinations, especially the MRI and PET scan results. Although the affected members of these two families had similar symptoms, such as quadrupedal palmigrade locomotion and retarded cognitive abilities including language, Barany's caloric nystagmus test indicated that they had different etiologies: central vestibular damage in the first family and peripheral vestibular damage in the second. Accordingly, the MRI and PET scans showed different results: cerebellar and vermial atrophy with considerably lowered metabolic activity in the first family, and quasi-normal MRI and PET scans in the second. These results suggest that the vestibulo-cerebellar system may be responsible for the cognitive retardation, whereas the quadrupedal gait may have different origins, such as developmental delay in the transition from quadrupedality into bipedality during babyhood. The higher brain networks suppressing the quadrupedal walking mechanisms and creating a bipedal walking system may be absent from individuals who prefer the quadrupedal walking style instead of the normal bipedal walking style. The quadrupedal individuals, live models instead of fossils, may be important for understanding the transition from quadrupedality to bipedality in human evolution.

REFERENCES

Bense, S., Deutschlaender, A., Stephan, Th., Bartenstein, P., Schwaiger, M., Brandt, Th., & Dieterich, M. (2004). Preserved visual-vestibular interaction in patients with Bilateral Vestibular failure. *Neurology*, *63*, 122–128.

Earhart, G. M., & Bastian, A. J. (2001). Cerebellar gait ataxia: Selection and coordination of human locomotor forms. *Journal of Neurophysiology*, *85*, 759–769.

Fiez, J. A., Peterson, S. E., Cheney, M. K., & Raichle, M. E. (1992). Impaired non-motor learning and error detection associated with cerebellar damage. A single case study. *Brain*, *115*, 155–178.

Leiner, H. C., Leiner, A. L., & Dow, R. S. (1993). Cognitive and language functions of the human cerebellum. *Trends in Neurosciences*, *16*, 444–447.

Leiner, H. C., Leiner, A. L., & Dow, R. S. (1995). The underestimated cerebellum. *Human Brain Mapping*, *2*, 244–254.

Porter, M. L., & Crandall, K. A. (2003). Lost along the way: The significance of evolution in reverse. *Trends in Ecology and Evolution*, *18*, 541–547.

Schmahmann, J. D. (1991). An emergent concept: Cerebellar contribution to higher function. *Archives of Neurology*, *48*, 1178–1187.

Schmahmann, J. D. (1996). From movement to thought: Anatomic substrates of the cerebellar contribution to cognitive processing. *Human Brain Mapping*, *4*, 174–198.

Tan, U. (2005a). Unertan sendromu ve insan ruhunun evrimine iliskin yeni bir teori. *Biyobank*,e.B.D. 2

Tan, U. (2005b). A new theory on the evolution of human mind; Unertan syndrome: Quadrupedality, primitive language, and severe mental retardation. *Neuroquantology*, *4*, 250–255.

Tan, U. (2006a). A new syndrome with quadrupedal gait, primitive speech, and severe mental retardation as a live model for human evolution. *International Journal of Neuroscience*, *116*, 361–370.

Tan, U. (2006b). Evidence for "Unertan syndrome" and the evolution of the human mind. *International Journal of Neuroscience*, *116*, 763–774.

Tan, U. (2006c). Evidence for Uner Tan Syndrome as a human model for reverse evolution. *International Journal of Neuroscience*, *116*, 1539–1547.

Tan, U. (2007). A wrist-walker exhibiting no "Uner Tan Syndrome.". *International Journal of Neuroscience*, *117*, 147–156.

Tan, U., Tan, M., Polat, P., Ceylan, Y., Suma, S., & Okur, A. (1999). Magnetic resonance imaging brain size/IQ relations in Turkish university students. *Intelligence*, *27*, 83–92.

Turkmen, S., Demirhan, O., Hoffmann, K., Diers, A., Zimmer, C., Sperling, K., & Mundlos, S. (2006). Cerebellar hypoplasia and quadrupedal locomotion in humans as a recessive trait mapping to chromosome 17p. *Journal of Medical Genetics*, *43*, 461–464.